

A Decentralized Optimal Control Framework for Connected and Automated Vehicles at Urban Intersections

Andreas A. Malikopoulos, Christos G. Cassandras, Yue J. Zhang

Abstract—We address the problem of optimally controlling connected automated vehicles (CAVs) crossing an urban intersection without any explicit traffic signaling. We first formulate a centralized problem with the objective of controlling CAV acceleration/deceleration to maximize traffic throughput subject to hard safety constraints and minimal energy cost. We show that the solution of this problem provides the times required for individual CAVs to cross the intersection and that the centralized problem becomes, under certain conditions, equivalent to a decentralized framework whereby each CAV minimizes its energy consumption subject to the throughput-maximizing timing constraints. We present a complete analytical solution of these decentralized problems and derive conditions under which feasible solutions satisfying all safety constraints always exist. The effectiveness of the proposed solution is validated through simulation and shows significant reductions in both fuel consumption and travel time.

Index Terms—Connected and automated vehicles, decentralized optimal control, autonomous intersections, traffic flow, motion planning, energy usage, safety.

I. INTRODUCTION

NEXT generation transportation systems are typical cyber-physical systems where discrete event-driven components monitor and control online physical entities. We are currently witnessing an increasing integration of energy, transportation, and cyber networks, which, coupled with human interactions, is giving rise to a new level of complexity in the transportation network and necessitates new control and optimization approaches.

The alarming state of current transportation systems is well documented. For example, in 2014, congestion caused people in urban areas to spend 6.9 billion hours more on

This manuscript has been authored by UT-Battelle, LLC under Contract No. DE-AC05-00OR22725 with the U.S. Department of Energy. The United States Government retains and the publisher, by accepting the article for publication, acknowledges that the United States Government retains a non-exclusive, paid-up, irrevocable, world-wide license to publish or reproduce the published form of this manuscript, or allow others to do so, for United States Government purposes.

This research was supported in part by the Laboratory Directed Research and Development Program of the Oak Ridge National Laboratory, Oak Ridge, TN 37831 USA, managed by UT-Battelle, LLC, for the US Department of Energy (DOE), and in part by UT-Battelle, LLC, through DOE contract DE-AC05-00OR22725 under DOE's SMART Mobility Initiative. The work of Cassandras and Zhang is supported in part by NSF under grants CNS-1239021, ECCS-1509084, and IIP-1430145, by AFOSR under grant FA9550-15-1-0471, and by The MathWorks.

A.A. Malikopoulos is with the Energy & Transportation Science Division, Oak Ridge National Laboratory, Oak Ridge, TN 37831 USA (e-mail: andreas@ornl.gov).

C.G. Cassandras and Y.J. Zhang are with the Division of Systems Engineering and Center for Information and Systems Engineering, Boston University, Boston, MA 02215 USA (e-mail: cgc@bu.edu; joycecz@bu.edu).

the road and to purchase an extra 3.1 billion gallons of fuel, resulting in a total cost estimated at \$160 billion [1]. From a control and optimization standpoint, the challenge is to develop mechanisms that expand capacity *without* affecting the existing road infrastructure, specifically by tighter spacing of vehicles in roadways and better control at the weakest links of a transportation system: the bottleneck points defined by intersections, merging roadways, and speed reduction zones, combined with the driver responses to various disturbances [2], [3]. An automated highway system (AHS) can alleviate congestion, reduce energy use and emissions, and improve safety by significantly increasing traffic flow as a result of closer packing of automatically controlled vehicles. Forming “platoons” of vehicles traveling at high speed is a popular system-level approach to address traffic congestion that gained momentum in the 1980s and 1990s [4], [5]. More recently, a study [6] indicated that transitioning from intersections with traffic lights to autonomous intersections, where vehicles can coordinate and cross the intersection without the use of traffic lights, has the potential of doubling capacity and reducing delays.

Connected and automated vehicles (CAVs) provide the most intriguing opportunity for enabling users to better monitor transportation network conditions and to improve traffic flow. CAVs can be controlled at different transportation segments, e.g., intersections, merging roadways, roundabouts, speed reduction zones and can assist drivers in making better operating decisions to improve safety and reduce pollution, energy consumption, and travel delays. One of the very early efforts in this direction was proposed in 1969 by Athans [7] for safe and efficient coordination of merging maneuvers with the intention of avoiding congestion. Assuming a given merging sequence, the merging problem was formulated as a linear optimal regulator [8] to control a single string of vehicles, with the aim of minimizing the speed errors that will affect the desired headway between each consecutive pair of vehicles. Varaiya [9] has also discussed extensively the key features of an automated intelligent vehicle-highway system (IVHS) and proposed a related control system architecture.

In this paper, we address the problem of coordinating on line a number of CAVs crossing an urban intersection with no traffic light signaling. The objective is to optimally control the acceleration/deceleration of each vehicle to minimize fuel consumption under hard safety constraints to avoid rear-end and lateral collisions, while also seeking to maximize the traffic throughput at the intersection. Several research efforts have been reported in the literature proposing either

centralized or decentralized approaches on coordinating CAVs at intersections. In this paper, we categorize an approach as centralized if there is at least one task in the system that is globally decided for all vehicles by a single central controller. In decentralized approaches, each vehicle obtains information from other vehicles and roadside infrastructure to optimize specific performance criteria (e.g., efficiency, travel time) while satisfying the transportation system’s physical constraints (e.g., stop signs, traffic signals). Dresner and Stone [10] proposed the use of a centralized reservation scheme to control a single intersection of two roads with vehicles traveling with similar speed on a single direction on each road, i.e., no turns are allowed. In their approach, each vehicle is treated as an agent who requests the reservation of the space-time cells to cross the intersection at a particular time interval defined from the estimated arrival time at the intersection. Since then, numerous centralized approaches have been reported in the literature [11]–[13] to achieve safe and efficient control of traffic through intersections. Some approaches have focused on coordinating vehicles at intersections to improve the travel time [14]–[16]. Others have considered minimizing the overlap in the position of vehicles inside the intersection, rather than arrival time [17]. Kim and Kumar [18] proposed an approach based on Model Predictive Control (MPC) that allows each vehicle to optimize its movement locally in a distributed manner with respect to any objective of interest. Miculescu and Karaman [19] used queueing theory and modeled the problem as a polling system with two queues and one server that determines the sequence of times assigned to the vehicles on each road.

In decentralized approaches, each vehicle determines its own control policy based on the information received from other vehicles on the road or from a coordinator. Alonso et al. [20] proposed two conflict resolution schemes in which an autonomous vehicle can make a decision about the appropriate schedule of crossing the intersection to avoid collision with other manually driven vehicles. Colombo and Del Vecchio [21] constructed the invariant set for the control inputs that ensure lateral collision avoidance. A decentralized optimal control framework whose solution yields the optimal acceleration/deceleration of a vehicle at any time in the sense of minimizing fuel consumption was presented in [22]. A detailed discussion of the research efforts in this area that have been reported in the literature to date can be found in [23].

The contributions of this paper are as follows. First, we formulate a centralized optimal control problem and establish that (i) the safety constraints dictate the time for each vehicle to cross the intersection by forming a first-in-first-out (FIFO) queue with this time dependent only on the preceding vehicle’s state; (ii) once the time for each vehicle to cross the intersection is determined, the centralized problem becomes, under certain conditions, equivalent to a decentralized framework over all CAVs in this FIFO queue. In this decentralized framework, the analytical solution of each CAV’s optimal control problem without considering state and control constraints was presented in [24] and [25] for coordinating online CAVs at

highway on-ramps, and in [22] for two adjacent intersections. Here, we present a complete analytical solution that includes all state and control constraints. Ensuring that a *feasible* solution to each CAV decentralized optimal control problem exists is nontrivial. Thus, another contribution is showing that this solution depends on the arrival time of a CAV at a “control zone” defined for the intersection and on its initial speed and then proving the existence of a nonempty feasibility region in the space defined by this arrival time and initial speed. Finally, we validate the effectiveness of the proposed solution by simulating the operation of a single intersection, and we show that coordination of CAVs can reduce significantly both fuel consumption and travel time.

The paper is organized as follows. In Section II, we introduce the modeling framework, present the assumptions of our approach and formulate the centralized optimal control problem. In Section III, we present the solution of the centralized problem and show how to convert it into a set of decentralized problems, one for each CAV. In Section IV, we derive a closed-form analytical solution for each decentralized problem and show the existence of feasible solutions ensuring that the rear-end collision constraint does not become active. Finally, we provide simulation results in Section V and concluding remarks in Section VI.

II. PROBLEM FORMULATION

A. Vehicle Model, Constraints, and Assumptions

We consider an intersection (Fig. 1) where the region at the center of the intersection is called *Merging Zone* (MZ) and is the area of potential lateral collision of the vehicles. Although this is not restrictive, we consider the MZ to be a square of side S . The intersection has a *Control Zone* (CZ) and a coordinator that can communicate with the vehicles traveling inside the CZ. Note that the coordinator is not involved in any decision for any CAV and only enables communication of appropriate information among CAVs.

The distance from the entry of the CZ to the entry of the MZ is L and it is assumed to be the same for all CZ entry points. The value of L depends on the coordinator’s communication range capability with the CAVs, while S is the physical length of a typical intersection. We do not allow CAV lane changes at the MZ and limit ourselves in this paper to the case of no turns allowed.

Let $N(t) \in \mathbb{N}$ be the number of CAVs inside the CZ at time $t \in \mathbb{R}^+$ and let $\mathcal{N}(t) = \{1, \dots, N(t)\}$ be a FIFO queue where i uniquely identifies a CAV’s order in the FIFO queue. Note that $N(t)$ is increasing in t and can be reset to $N(t) = 0$ only if no vehicles are inside the CZ. For simplicity, we represent the dynamics of each CAV $i \in \mathcal{N}(t)$, moving along a specified lane through second order dynamics

$$\begin{aligned} \dot{p}_i &= v_i(t), & p_i(t_i^0) &= 0 \\ \dot{v}_i &= u_i(t), & v_i(t_i^0) &\text{ given} \end{aligned} \quad (1)$$

where t_i^0 is the time when CAV i enters the CZ, and $p_i(t) \in \mathcal{P}_i$, $v_i(t) \in \mathcal{V}_i$, $u_i(t) \in \mathcal{U}_i$ denote the position, speed and

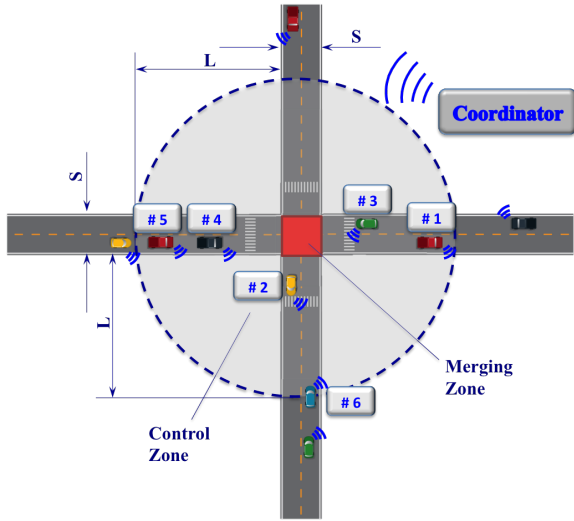


Fig. 1. Intersection with connected and automated vehicles.

acceleration/deceleration (control input) of each CAV i inside the CZ. The sets \mathcal{P}_i , \mathcal{V}_i and \mathcal{U}_i , $i \in \mathcal{N}(t)$, are complete and totally bounded subsets of \mathbb{R} . The state space $\mathcal{P}_i \times \mathcal{V}_i$ is closed with respect to the induced topology, thus, it is compact.

We need to ensure that for any initial time and state (t_i^0, p_i^0, v_i^0) and every admissible control $u(t)$, the system (1) has a unique solution $(p_i(t), v_i(t))$ on some interval $[t_i^0, t_i^m]$, where t_i^m is the time that vehicle $i \in \mathcal{N}(t)$ enters the MZ. To ensure that the control input and vehicle speed are within a given admissible range, the following constraints are imposed:

$$\begin{aligned} u_{i,min} &\leq u_i(t) \leq u_{i,max}, \quad \text{and} \\ 0 &\leq v_{min} \leq v_i(t) \leq v_{max}, \quad \forall t \in [t_i^0, t_i^m], \end{aligned} \quad (2)$$

where $u_{i,min}$, $u_{i,max}$ are the minimum and maximum control inputs (maximum deceleration/acceleration) for each vehicle $i \in \mathcal{N}(t)$, and v_{min} , v_{max} are the minimum and maximum speed limits respectively. For simplicity, in the sequel we do not consider vehicle diversity and thus set $u_{i,min} = u_{min}$ and $u_{i,max} = u_{max}$.

To ensure the absence of any rear-end collision of two consecutive vehicles traveling on the same lane, the position of the preceding vehicle should be greater than or equal to the position of the following vehicle plus a predefined safe distance $\delta < S$. Thus, we impose the rear-end safety constraint

$$s_i(t) = p_k(t) - p_i(t) \geq \delta, \quad \forall t \in [t_i^0, t_i^m], \quad (3)$$

where we will reserve the symbol k to denote the vehicle which is physically immediately ahead of i in the same lane.

Definition 1: For each vehicle $i \in \mathcal{N}(t)$, we define the set Γ_i that includes only the positions along the lane where a lateral collision is possible, namely

$$\Gamma_i \triangleq \left\{ p_i(t) \mid p_i(t) \in [L, L + S], \forall t \in [t_i^m, t_i^f] \right\}. \quad (4)$$

where t_i^f is the time that vehicle $i \in \mathcal{N}(t)$ exits the MZ.

To avoid a lateral collision for any two vehicles $i, j \in \mathcal{N}(t)$ on different roads, the following constraint should hold

$$\Gamma_i \cap \Gamma_j = \emptyset, \forall t \in [t_i^m, t_i^f]. \quad (5)$$

The above constraint implies that only one vehicle at a time can be inside the MZ. If the length of the MZ is long, then this constraint might not be realistic since it results in dissipating space and capacity of the road. However, the constraint is not restrictive in the problem formulation and it can be modified appropriately as described in the following section.

In the modeling framework described above, we impose the following assumptions:

Assumption 1: For CAV i , none of the constraints (2)-(3) is active at t_i^0 .

Assumption 2: The speed of the CAVs inside the MZ is constant, i.e., $v_i(t) = v_i(t_i^m) = v_i(t_i^f)$, $\forall t \in [t_i^m, t_i^f]$. This implies that

$$t_i^f = t_i^m + \frac{S}{v_i(t_i^m)}. \quad (6)$$

Assumption 3: Each CAV i has proximity sensors and can measure local information without errors or delays.

We briefly comment on the above assumptions. The first assumption ensures that the initial state and control input are feasible. The second assumption is intended to enhance safety awareness, but it could be modified appropriately, if necessary, as discussed in Section III. The third assumption may be a strong requirement to impose, but it is relatively straightforward to extend our results in the case that it is relaxed as long as the noise in the measurements and/or delays are bounded. For example, we can determine upper bounds on the state uncertainties as a result of sensing or communication errors and delays, and incorporate these into more conservative safety constraints.

B. Centralized Problem Formulation

We begin by considering the acceleration/deceleration of each CAV i which minimizes the following cost functional:

$$J_i(u_i(t), t_i^m) = \int_{t_i^0}^{t_i^m} C_i(u_i(t)) dt, \quad (7)$$

$$\begin{aligned} \text{subject to : } & (1), (2), p_i(t_i^0) = 0, p_i(t_i^m) = L, \text{ and} \\ & \text{given } t_i^0, v_i(t_i^0), t_i^m, v_i(t_i^m), \end{aligned}$$

where $C_i(\cdot)$ is a monotonically increasing function of its argument and such that $C_i(0) = 0$. Note that the L^2 -norm of the control input in $[t_i^0, t_i^m]$ is a special case with $C_i(u_i(t)) = \frac{1}{2}u_i^2(t)$. Recall that under Assumption 2, the CAV is cruising in the MZ, so that $u_i(t) = 0$ for $t \in [t_i^m, t_i^f]$. Thus, there is no need to include $[t_i^m, t_i^f]$ in (7) above. In this problem, a CAV is required to travel through a CZ of length L under given initial and terminal conditions. We assume that t_i^0 , $v_i(t_i^0)$ are given, but t_i^m depends on the additional constraints (3) and (5) not included above. Thus, we view a solution of this problem as being parameterized by t_i^m and express it as $u_i(t; t_i^m)$. Solutions $u_i(t; t_i^m)$ of (7) define a set of controls as follows:

$$\begin{aligned} \mathcal{A}_i &\triangleq \left\{ u_i \in \mathcal{U}_i \mid u_i(t; t_i^m) = \arg \min J_i(u_i(t), t_i^m), \right. \\ &\text{subject to : (1), (2), } p_i(t_i^0) = 0, p_i(t_i^m) = L, \\ &\left. \text{and given } t_i^0, v_i(t_i^0), t_i^m, v_i(t_i^m) \right\}. \end{aligned}$$

We now turn our attention to the problem of maximizing the traffic throughput at the intersection (see Fig. 1) under the hard safety constraints imposed to avoid rear-end collision and to cross the intersection without lateral collision. We will seek to maximize the throughput with the control input (acceleration/deceleration) in the set \mathcal{A}_i for each CAV i . The first CAV in every FIFO queue $\mathcal{N}(t)$, created inside the CZ over time, is unconstrained since none of the safety constraints, (3) and (5), can become active. Thus, the optimal solution for CAV #1, $u_1(t; t_1^m) \in \mathcal{A}_1$, is to cruise inside the CZ with zero acceleration/deceleration (e.g., constant speed), i.e., $u_1(t) = 0$, for all $t \in [t_1^0, t_1^f]$. The FIFO structure imposes the following condition:

$$t_i^m \geq t_{i-1}^m, \quad \forall i \in \mathcal{N}(t), \quad i > 1. \quad (8)$$

In view of the set \mathcal{A}_i and (8), setting $\mathbf{t}_{(2:N(t))} = [t_2^m \dots t_{N(t)}^m]$ and $\mathbf{u}_{(1:i)}(t) = [u_1(t; t_1^m) \dots u_i(t; t_i^m)]$, for every FIFO queue $\mathcal{N}(t)$ created inside the CZ over time, the centralized control problem can be formulated as follows:

Centralized Problem:

$$\begin{aligned} \min_{\mathbf{t}_{(2:N(t))}} & \sum_{i=2}^{N(t)} \left(t_i^m(\mathbf{u}_{(1:i)}(t)) - t_{i-1}^m(\mathbf{u}_{(1:i-1)}(t)) \right) \\ & = \min_{\mathbf{t}_{N(t)}} \left(t_{N(t)}^m(\mathbf{u}_{(1:N(t))}(t)) - t_1^m(\mathbf{u}_{(1)}(t)) \right), \quad (9) \end{aligned}$$

subject to : $u_i(t; t_i^m) \in \mathcal{A}_i, \quad \forall i \in \mathcal{N}(t)$, (3), (5), and (8).

The equivalence between the two expressions in (9) (due to the cancellation of all terms in the sum except the first and last) reflects the equivalence between minimizing the total time to process all CAVs in the FIFO queue and the average interarrival time of CAVs at the MZ.

From a practical point of view, there are substantial potential benefits to the solution of (9). Vehicles will not have to come to a full stop at the intersection, thereby conserving momentum and fuel while also improving travel time. Moreover, by optimizing CAV acceleration/deceleration, we minimize transient engine operation, thus we can have direct benefits in fuel consumption [25] and emissions since internal combustion engines are optimized over steady state operating points (constant torque and speed) [26].

The computational requirements associated with deriving the optimal solution of (9) with the minimum acceleration/deceleration of each CAV, i.e., $u_i(t; t_i^m) \in \mathcal{A}_i$, for all $i \in \mathcal{N}(t)$, can make online implementation in CAVs really challenging. In addition, having a centralized controller with demanding computational capabilities at each intersection is clearly not cost-effective. Thus, we seek a decentralized framework that solves (9) at the individual CAV level by

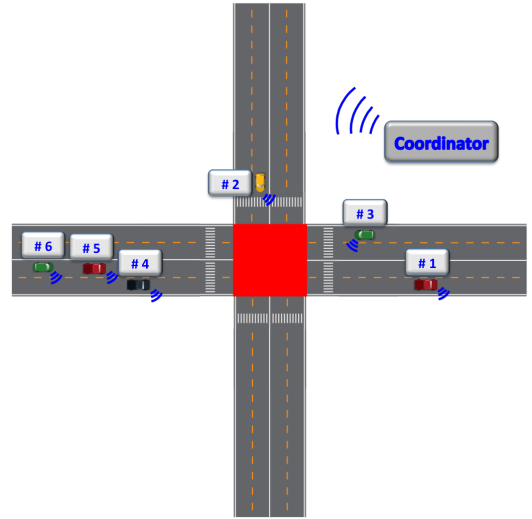


Fig. 2. Intersection with connected and automated vehicles with different directions.

imposing an information exchange communication structure among vehicles and with the coordinator as discussed next. What is important to observe in (9) is that the constraints (3), (5), and (8) directly affect the admissible set for each t_i^m in $\mathbf{t}_{(2:N(t))}$ and, ultimately, the actual selection of t_i^m . We will show in the next section that this facilitates the determination of a solution $\mathbf{t}_{(2:N(t))}^* = [t_2^{m*} \dots t_{N(t)}^{m*}]$, hence also $v_i(t_i^{m*})$ and $u_i^*(t; t_i^{m*})$ solving (7) for all $i = 1, \dots, N(t)$.

III. VEHICLE COMMUNICATION STRUCTURE

A. Terminal Condition Determination

We begin by subdividing the FIFO queue $\mathcal{N}(t)$ into subsets as follows.

Definition 2: Each CAV $i \in \mathcal{N}(t)$ belongs to at least one of the following four subsets of $\mathcal{N}(t)$ depending on its physical location inside the CZ: 1) $\mathcal{R}_i(t)$ contains all CAVs traveling on the same road as i and towards the same direction but on different lanes (e.g., CAVs # 4 and # 5 in Fig. 2), 2) $\mathcal{L}_i(t)$ contains all CAVs traveling on the same road and lane as vehicle i (e.g., CAVs # 5 and # 6 in Fig. 2), 3) $\mathcal{C}_i(t)$ contains all CAVs traveling on different roads from i and having destinations that can cause collision at the MZ, (e.g., CAVs # 2 and # 3 in Fig. 2), and 4) $\mathcal{O}_i(t)$ contains all CAVs traveling on the same road as i and opposite destinations that cannot, however, cause collision at the MZ (e.g., CAVs # 3 and # 4 in Fig. 2).

We now consider the following possible cases regarding any CAV i as it enters the CZ:

Case 1: $(i-1) \in \mathcal{R}_i(t) \cup \mathcal{O}_i(t)$: in this case, none of the safety constraints (3) and (5) can become active while i and $i-1$ are in the CZ or MZ. This allows CAV i to minimize its time in the CZ while preserving the FIFO queue through (8). Therefore, it is obvious that we should set

$$t_i^m = t_{i-1}^m \quad (10)$$

and since CAV speeds inside the MZ are constant (Assumption 2), both $i-1$ and i will also be exiting the MZ at the same time by setting

$$v_i(t_i^m) = v_{i-1}(t_{i-1}^m). \quad (11)$$

Note that, by Assumption 2, $v_i(t) = v_{i-1}(t)$ for all $t \in [t_i^m, t_i^f]$.

Case 2: $(i-1) \in \mathcal{L}_i(t)$: in this case, only the rear-end collision constraint (3) can become active. In order to minimize the time CAV i spends in the CZ by ensuring that (3) and (8) are both satisfied over $t \in [t_i^m, t_{i-1}^f]$ while $v_{i-1}(t)$ is constant (Assumption 2), we set

$$t_i^m = t_{i-1}^m + \frac{\delta}{v_{i-1}(t_{i-1}^m)}, \quad (12)$$

and $v_i(t_i^m)$ as in (11).

Case 3: $(i-1) \in \mathcal{C}_i(t)$: in this case, only the lateral collision constraint (5) can become active. Hence, CAV i is allowed to enter the MZ only when vehicle $i-1$ exits from it. To minimize the time CAV i spends in the CZ while ensuring that (8) holds and (5) is satisfied over $t \in [t_i^m, t_{i-1}^f]$, we set

$$t_i^m = t_{i-1}^m + \frac{S}{v_{i-1}(t_{i-1}^m)}, \quad (13)$$

and $v_i(t_i^m)$ as in (11).

It follows from (10) through (13) that t_i^m is always recursively determined from t_{i-1}^m and $v_{i-1}(t_{i-1}^m)$. Similarly, $v_i(t_i^m)$ depends only on $v_{i-1}(t_{i-1}^m)$. Clearly, there is more than one option for the desired speed $v_i(t_i^m)$ and the choices above are not restrictive to the solution of the centralized problem. It is important to note that (10) through (13) are only concerned with the specification of $v_i(t_i^m)$ at $t = t_i^m$. In particular, in *Cases 2-3*, (12) and (13) apply only to $t = t_i^m$ and do not impose any constraints on $v_i(t)$ for $t \in [t_{i-1}^m, t_i^m]$. Therefore, the safety constraint (3) may not hold over this interval and needs to be separately enforced in solving (9).

Remark 1: The lateral collision constraint (5) allows only one CAV at a time to be inside the MZ. If the length of the MZ is long, however, then this constraint may become overly conservative, since it results in dissipating space and road capacity. The constraint can be modified appropriately and (13) in *Case 3* above can be rewritten as

$$t_i^m = t_{i-1}^m + \frac{r}{v_{i-1}(t_{i-1}^m)} \quad (14)$$

with any desired distance $r < S$ between CAVs within the MZ.

Although (10), (12), and (13) provide a simple recursive structure for determining t_i^m , the presence of the control and state constraints (2) may prevent these values from being admissible. This may happen by (2) becoming active at some internal point during an optimal trajectory of (9) and we will analyze such cases based on the properties of the optimal control that we will derive in Section IV. In addition, however, there is a global lower bound to t_i^f , hence also t_i^m through (6), which depends on t_i^0 and v_i^0 that can be determined as follows. This lower bound depends on whether CAV i can

reach v_{max} prior to t_{i-1}^m or not: (i) If CAV i enters the CZ at t_i^0 , accelerates with u_{max} until it reaches v_{max} and then cruises at this speed until it leaves the MZ at time t_i^1 , it was shown in [22] that

$$t_i^1 = t_i^0 + \frac{L+S}{v_{max}} + \frac{(v_{max} - v_i^0)^2}{2u_{max}v_{max}}. \quad (15)$$

(ii) If CAV i accelerates with u_{max} but reaches the MZ at t_i^m with speed $v_i(t_i^m) < v_{max}$, it was shown in [22] that

$$t_i^2 = t_i^0 + \frac{v_i(t_i^m) - v_i^0}{u_{max}} + \frac{S}{v_i(t_i^m)}. \quad (16)$$

where $v_i(t_i^m) = \sqrt{2Lu_{max} + (v_i^0)^2}$. Thus, $t_i^c = \max\{t_i^1, t_i^2\}$ is a lower bound of t_i^f regardless of the solution of (9). Therefore, we can summarize the recursive construction of t_i^f over $i = 1, \dots, N(t)$ as follows:

$$t_i^f = \begin{cases} t_1^f, & \text{if } i = 1, \\ \max\{t_{i-1}^f, t_i^c\}, & \text{if } i-1 \in \mathcal{R}_i(t) \cup \mathcal{O}_i(t) \\ \max\{t_{i-1}^f + \frac{\delta}{v_i(t_{i-1}^f)}, t_i^c\}, & \text{if } i-1 \in \mathcal{L}_i, \\ \max\{t_{i-1}^f + \frac{S}{v_i(t_{i-1}^f)}, t_i^c\}, & \text{if } i-1 \in \mathcal{C}_i, \end{cases} \quad (17)$$

where t_i^m can be evaluated from t_i^f through (6). Recall that t_1^f above is unconstrained by any prior CAVs and can be determined by setting $v_1(t) = v_1(t_1^0)$ for all $t \in [t_1^0, t_1^f]$, which obviously minimizes (7) since it implies that $u_1(t) = 0$ for all $t \in [t_1^0, t_1^f]$.

B. Solution of the Centralized Problem Formulation

The recursive structure in MZ entry times t_i^m that was established through (17) and (6) for all CAVs i in the FIFO queue $\mathcal{N}(t)$ is inherited by the optimal solution of the centralized problem (9) as formally shown next.

Lemma 1: Let $\mathbf{t}^* = [t_2^{m*}, \dots, t_N^{m*}]$ be a solution of the centralized problem (9) for N CAVs. Then, for all $i = 2, \dots, N$, $t_i^{m*}(u_{(1:i)}(t))$ can be recursively determined as a function of $t_{i-1}^{m*}(u_{(1:i-1)}(t))$, i.e., t_i^{m*} can be expressed as $t_i^{m*} = f_i(t_{i-1}^{m*})$.

Proof: For $N = 1$, t_1^{m*} can be determined without any constraints since it pertains to the only CAV in the CZ by setting, for instance, $v_1(t) = v_i(t_1^0)$ for all $t \in [t_1^0, t_1^m]$.

For any $N(t) > 1$, either (10), (12) or (13) applies with $i = N(t)$ and $i-1 = N(t)-1$, depending on which subset of the queue $N(t)$ belongs to. In addition, using (11) and the second form of (9) it immediately follows that for any $N(t)$ we have $t_{N(t)}^{m*} = f_{N(t)}(t_{N(t)-1}^{m*})$. ■

Theorem 1: The optimal MZ entry times $\mathbf{t}^* = [t_1^{m*}, \dots, t_N^{m*}]$ in the centralized problem (9) can be explicitly determined as a function of t_{i-1}^{m*} and $v_{i-1}(t_{i-1}^{m*})$.

The proof of the Theorem is basically repeating the iterative process in (10) through (13) and (17) and Lemma 1 over all $i = 2, \dots, N(t) \in \mathcal{N}(t)$, where $t_1^{m*}(u_{(1)}(t))$ and $v_1(t_1^{m*})$ are known.

Intuitively, the conclusion of this analysis is that the minimum time t_i^{m*} for each vehicle i to enter the MZ is dictated

by the FIFO queue and the safety constraints as designated through (10), (12) and (13). Once t_i^{m*} , and hence t_i^{f*} through (6), is determined, then we can optimize any function of the control input from the time t_i^0 that CAV i enters the CZ until it enters the MZ at t_i^{m*} . The following result formalizes this conclusion.

Theorem 2: Let $\mathbf{t}^* = [t_2^{m*}(u_1(t)), \dots, t_{N(t)}^{m*}(u_{(1:N(t)}(t))]$ be the solution of the centralized problem (9) for $N(t)$ vehicles. Then, $[u_1(t; t_1^{m*}), \dots, u_{N(t)}(t; t_{N(t)}^{m*})]$, $t \in (t_i^0, t_i^{m*})$, $i = 2, \dots, N(t)$, is also a solution of the decentralized problems in (7) with the cost functional $J_i(u_i(t), t_i^{m*})$.

Proof: Since $t_i^{m*}(u_{(1:i)}(t))$ is an entry of the vector \mathbf{t}^* , it follows that $u_i(t; t_i^{m*}) \in \mathcal{A}_i$ for all $i = 2, \dots, N$. Therefore, by the definition of \mathcal{A}_i , $u_i(t; t_i^{m*})$ is a solution of (7). ■

Remark 2: Note that the optimal solution \mathbf{t}^* guarantees that the safety constraints (3) and (5) do not become active in $[t_1^0, t_N^f]$, assuming they are not active at $t = t_i^0$ (Assumption 1) for all $i = 1, \dots, N$. On the other hand, solutions $u_1^*(t; t_1^m), \dots, u_N^*(t; t_N^m)$ of the decentralized problems in (7) with t_i^m , $i = 1, \dots, N$, evaluated using (10) through (17) satisfy $u_i^*(t; t_i^m) \in \mathcal{A}_i$ and, therefore, $t_i^m(u_1^*(t; t_1^m), \dots, u_N^*(t; t_N^m))$, $i = 1, \dots, N$, may also be solutions of the centralized problem (9), but only if they satisfy the constraints (3) and (5) included in (9). The latter constraint is satisfied since t_i^m and $v_i(t_i^m)$ in (11) and (13) are specifically selected for this purpose. On the other hand, the former is not guaranteed to hold for all $t \in [t_i^0, t_i^m]$. In fact, as we will discuss in Section IV-C, it is easy to show that this may not hold depending on the initial conditions (t_i^0, v_i^0) for CAV i . We will show, however, in Theorem 3 that there exists a nonempty feasible region $\mathcal{F}_i \subset R^2$ of initial conditions (t_i^0, v_i^0) such that $s_i(t) \geq \delta$ for all $t \in (t_i^0, t_i^m)$.

IV. DECENTRALIZED FRAMEWORK

A. Decentralized Communication Structure

The results in the previous section allow us to address the centralized problem within a decentralized framework, in which each CAV can solve the optimal control problem (7). However, to establish this decentralized framework, we need a communication structure between CAVs with a “coordinator” whose task is to handle the information between CAVs. In particular, when a CAV i reaches the CZ of the intersection at some instant t , the coordinator assigns to it a unique identity as follows.

Definition 3: The *unique identity* that the coordinator assigns to each CAV $i \in \mathcal{N}(t)$, is a pair (i, j) where $i = N(t) + 1$ is an integer representing the order of the vehicle in the FIFO queue $\mathcal{N}(t)$ and $j \in \{1, \dots, 4\}$ is an integer based on a one-to-one mapping from $\{\mathcal{R}_i(t), \mathcal{L}_i(t), \mathcal{C}_i(t), \mathcal{O}_i(t)\}$ onto $\{1, \dots, 4\}$.

If two or more CAVs enter the CZ at the same time, then the coordinator selects their position in the queue according to their initial speed. For example, the CAV with the highest initial speed will be assigned the next available position i in the

queue, and so forth. If the CAVs enter the CZ at the same with the same initial speed, then the coordinator selects randomly their position in the queue.

Definition 4: For each vehicle i entering a CZ, we define the *information set* $Y_i(t)$ as

$$Y_i(t) \triangleq \left\{ p_i(t), v_i(t), \mathcal{Q}_i, s_i(t), t_i^m \right\}, \forall t \in [t_i^0, t_i^m], \quad (18)$$

where $p_i(t), v_i(t)$ are the position and speed of CAV i inside the CZ, $\mathcal{Q}_i \in \{1, \dots, 4\}$ is the queue subset (Definition 2) assigned to CAV i by the coordinator, and $s_i(t) = p_k(t) - p_i(t)$ is the distance between CAV i and some CAV k which is immediately ahead of i in the same lane (recall that we reserve the symbol k to denote such a CAV relative to i). The last element above, t_i^m , is the time targeted for CAV i to enter the MZ, whose evaluation was discussed in Section III and is given by one of (10), (12), (13) depending on the value of \mathcal{Q}_i or, to account for the lower bound derived on t_i^f , by (17).

Each vehicle $i \in \mathcal{N}(t)$ has proximity sensors and can observe and/or estimate the information in $Y_i(t)$ without errors or delays (Assumption 3). Note that once CAV i enters the CZ, then immediately all information in $Y_i(t)$ becomes available to i : $p_i(t), v_i(t)$ are read from its sensors; \mathcal{Q}_i is assigned by the coordinator, as is the value of k based on which $s_i(t)$ is also evaluated; t_i^m can also be computed at that time based on the information the vehicle i receives from $i - 1$. The recursion on t_i^m is initialized whenever a vehicle enters the CZ. In this case, t_i^m can be externally assigned as the desired exit time of this vehicle whose behavior is unconstrained (as discussed in the previous section). Thus, the time t_i^m is fixed and available through $Y_i(t)$.

Since the coordinator is not involved in any decision on the vehicle coordination, from Theorem 1 we can formulate $N(t)$ sequential decentralized tractable problems that may be solved on line. A special case of Theorem 1 arises when the cost function is the L^2 -norm of the control input in $[t_i^0, t_i^m]$. By minimizing the L^2 -norm of the control input, we minimize transient engine operation, thus we can have direct benefits in fuel consumption [25] and emissions since internal combustion engines are optimized over steady state operating points (constant torque and speed) [26]. Hence the decentralized problem for each vehicle i is formulated as follows:

$$\min_{u_i} \frac{1}{2} \int_{t_i^0}^{t_i^m} u_i^2(t) dt, \quad (19)$$

subject to : (1), (2), (6), (17), $p_i(t_i^0) = 0$, $p_i(t_i^m) = L$, and given $t_i^0, v_i(t_i^0)$.

Observe that, compared to (9), we have omitted the rear end safety constraint (3) and the lateral collision constraint (5). As mentioned earlier, the latter is implicitly handled by the selection of $v_i(t_i^m)$ and t_i^m in (13). The former is omitted because we will show that the solution of (19) guarantees that this constraint holds throughout $[t_i^0, t_i^m]$ (we also know it holds in $[t_i^m, t_i^f]$ as discussed in Section III-A). Thus, it is a simpler problem to solve online. The terminal time t_i^m can be

determined by (6) and (17), which preserves the FIFO queue, upon the CAV i entering the CZ since it depends only on info from $i - 1$.

B. Analytical solution of the decentralized optimal control problem

For the analytical solution of the decentralized problem (19) and its on line implementation, we apply Hamiltonian analysis. We have assumed (Assumption 1) that when the CAVs enter the CZ, none of the constraints is active. However, this is not in general true. For example, a CAV may enter the CZ with speed higher than the speed limit. In this case, a solution of the optimal control problem is infeasible. A feasibility analysis for CAVs to satisfy such initial conditions is discussed in Section IV-C where we show that a feasible region $\mathcal{F}_i \subset R^2$ of initial conditions (t_i^0, v_i^0) for CAV i exists such that $s_i(t) \geq \delta$ for all $t \in [t_i^0, t_i^m]$; a feasibility enforcement analysis to ensure the existence of feasible and optimal solutions is given in [27].

From (19), the state equations (1), and the control/state constraints (2), for each vehicle $i \in \mathcal{N}(t)$ the Hamiltonian function is

$$\begin{aligned} H_i(t, p(t), v(t), u(t)) &= \frac{1}{2}u_i^2 + \lambda_i^p \cdot v_i + \lambda_i^v \cdot u_i \\ &+ \mu_i^a \cdot (u_i - u_{max}) + \mu_i^b \cdot (u_{min} - u_i) + \mu_i^c \cdot (v_i - v_{max}) \\ &\quad + \mu_i^d \cdot (v_{min} - v_i), \end{aligned} \quad (20)$$

where λ_i^p and λ_i^v are the costates, and μ^T is a vector of Lagrange multipliers with

$$\mu_i^a = \begin{cases} > 0, & u_i(t) - u_{max} = 0, \\ = 0, & u_i(t) - u_{max} < 0, \end{cases} \quad (21)$$

$$\mu_i^b = \begin{cases} > 0, & u_{min} - u_i(t) = 0, \\ = 0, & u_{min} - u_i(t) < 0, \end{cases} \quad (22)$$

$$\mu_i^c = \begin{cases} > 0, & v_i(t) - v_{max} = 0, \\ = 0, & v_i(t) - v_{max} < 0, \end{cases} \quad (23)$$

$$\mu_i^d = \begin{cases} > 0, & v_{min} - v_i(t) = 0, \\ = 0, & v_{min} - v_i(t) < 0. \end{cases} \quad (24)$$

The Euler-Lagrange equations become

$$\dot{\lambda}_i^p = -\frac{\partial H_i}{\partial p_i} = 0, \quad (25)$$

and

$$\dot{\lambda}_i^v = -\frac{\partial H_i}{\partial v_i} = \begin{cases} -\lambda_i^p, & v_i(t) - v_{max} < 0 \text{ and} \\ & v_{min} - v_i(t) < 0, \\ -\lambda_i^p - \mu_i^c, & v_i(t) - v_{max} = 0, \\ -\lambda_i^p + \mu_i^d, & v_{min} - v_i(t) = 0, \end{cases} \quad (26)$$

with boundary conditions $p_i(t_i^0) = 0$, $p_i(t_i^m) = L$, given initial conditions t_i^0 , $v_i(t_i^0)$, and t_i^m , $v_i(t_i^m)$ specified by (6) and (17) in terms of t_{i-1}^m , $v_{i-1}(t_{i-1}^m)$.

The necessary condition for optimality is

$$\frac{\partial H_i}{\partial u_i} = u_i + \lambda_i^v + \mu_i^a - \mu_i^b = 0, \quad (27)$$

To address this problem, constrained and unconstrained arcs need to be pieced together to satisfy (25) through (27). We consider all possible such cases as follows.

1) *Control and State Constraints not Active:* In this case, which was presented in [24] and [25] for coordinating online CAVs at highway on-ramps, and in [22] at two adjacent intersections, we have $\mu_i^a = \mu_i^b = \mu_i^c = \mu_i^d = 0$. Applying (27), the optimal control is given by

$$u_i + \lambda_i^v = 0, \quad i \in \mathcal{N}(t). \quad (28)$$

and the Euler-Lagrange equations yield (25) and

$$\dot{\lambda}_i^v = -\frac{\partial H_i}{\partial v_i} = -\lambda_i^p. \quad (29)$$

From (25) we have $\lambda_i^p = a_i$ and (29) implies $\lambda_i^v = -(a_i t + b_i)$, where a_i and b_i are integration constants. Consequently, the optimal control input (acceleration/deceleration) as a function of time is given by

$$u_i^*(t) = a_i t + b_i. \quad (30)$$

Substituting this equation into the vehicle dynamics (1) we can find the optimal speed and position for each vehicle, namely

$$v_i^*(t) = \frac{1}{2}a_i t^2 + b_i t + c_i \quad (31)$$

$$p_i^*(t) = \frac{1}{6}a_i t^3 + \frac{1}{2}b_i t^2 + c_i t + d_i, \quad (32)$$

where c_i and d_i are integration constants. These constants can be computed by using the initial and final conditions in (19). Since we seek to derive the optimal control (30) on line, the integration constants can be viewed as functions of time and states, i.e., $a_i(t, p_i, v_i)$, $b_i(t, p_i, v_i)$, $c_i(t, p_i, v_i)$, and $d_i(t, p_i, v_i)$ and can be updated at each time t . It follows that (31) and (32), along with the initial and terminal conditions, can be used to form a system of four equations of the form $\mathbf{T}_i \mathbf{b}_i = \mathbf{q}_i$, namely

$$\begin{bmatrix} \frac{1}{6}t^3 & \frac{1}{2}t^2 & t & 1 \\ \frac{1}{2}t^2 & t & 1 & 0 \\ \frac{1}{6}(t_i^m)^3 & \frac{1}{2}(t_i^m)^2 & t_i^m & 1 \\ \frac{1}{2}(t_i^m)^2 & t_i^m & 1 & 0 \end{bmatrix} \cdot \begin{bmatrix} a_i \\ b_i \\ c_i \\ d_i \end{bmatrix} = \begin{bmatrix} p_i(t) \\ v_i(t) \\ p_i(t_i^m) \\ v_i(t_i^m) \end{bmatrix}, \quad (33)$$

where t_i^m is specified by (6) and (17), and $v_i(t_i^m)$ as discussed in Section III-A. Hence, we have

$$\mathbf{b}_i(t, p_i(t), v_i(t)) = (\mathbf{T}_i)^{-1} \cdot \mathbf{q}_i(t, p_i(t), v_i(t)), \quad (34)$$

where $\mathbf{b}_i(t, p_i(t), v_i(t))$ contains the four integration constants $a_i(t, p_i, v_i)$, $b_i(t, p_i, v_i)$, $c_i(t, p_i, v_i)$, $d_i(t, p_i, v_i)$. Thus, (30) can be written as

$$u_i^*(t, p_i(t), v_i(t)) = a_i(t, p_i(t), v_i(t))t + b_i(t, p_i(t), v_i(t)). \quad (35)$$

Since (33) can be computed on line, the controller can yield the optimal control online for each vehicle i , with feedback indirectly provided through the re-calculation of the vector $\mathbf{b}_i(t, p_i(t), v_i(t))$ in (34).

2) *Control Constraint Active, $u_i^*(t) = u_{max}$* : Suppose that at time $t = t_1$, (35) becomes equal to u_{max} while $v_{min} < v_i(t) < v_{max}$

$$u_i^*(t) = u_{max}, \forall t \geq t_1. \quad (36)$$

In this case the Hamiltonian is continuous at $t = t_1$ (entry point of the control constrained arc). Substituting the last equation into the vehicle dynamics equations (1) we can find the optimal speed and position of each vehicle, namely

$$v_i^*(t) = u_{max} t + f_i, \quad (37)$$

$$p_i^*(t) = \frac{1}{2} u_{max} t^2 + f_i t + e_i, \quad \forall t \geq t_1 \quad (38)$$

where f_i and e_i are constants of integration that can be computed easily since we know the speed and position of the vehicle at time $t = t_1$.

3) *Control and State Constraints Become Active, $u_i(t) = u_{max}$ and $v_i(t) = v_{max}$* : Suppose that at time $t = t_2 > t_1$ (exit point of the control constrained arc and entry point of the state variable constrained arc), $v_i^*(t)$ in (37) becomes equal to v_{max} . Then from (1) we have $\dot{v}_i^* = u_i^*(t) = 0$ for $t > t_2$, and the Hamiltonian is discontinuous at $t = t_2$ (corner). It follows from (1) that for $t \geq t_2$

$$v_i^*(t) = v_{max}, \quad (39)$$

$$p_i^*(t) = v_{max} t + r_i, \quad (40)$$

where r_i is the constant of integration that can be computed from the position of the vehicle at $t = t_2^-$.

Since $u_i^*(t) = 0$ for $t > t_2$, at time $t = t_3 > t_2$ (exit point of the corner) the state variable constraint can become inactive again, i.e., $v_{min} < v_i(t) < v_{max}$. The Hamiltonian and co-states are continuous at $t = t_3$, i.e., $H(t_3^-) = H(t_3^+)$, $\lambda_i^p(t_3^-) = \lambda_i^p(t_3^+) = g_i$, and $\lambda_i^v(t_3^-) = \lambda_i^v(t_3^+) = -(g_i t + h_i)$, where g_i and h_i are constants of integration. Hence

$$-\frac{1}{2} u_i^*(t) = g_i (v_{max} - v_i(t)). \quad (41)$$

The optimal control input, speed, and position are

$$u_i^*(t) = g_i t + h_i, \quad (42)$$

$$v_i^*(t) = \frac{1}{2} g_i t^2 + h_i t + q_i, \quad (43)$$

$$p_i^*(t) = \frac{1}{6} g_i t^3 + \frac{1}{2} h_i t^2 + q_i t + s_i, \quad (44)$$

where the constants of integration g_i , h_i , q_i , and s_i can be computed from the control, speed, and position of the vehicle at $t = t_3^-$ and (41) at $t = t_3^+$.

4) *Control Constraints Become Active, $u_i(t) = u_{min}$* : Suppose that at time $t = t_1$, (35) becomes equal to u_{min} while $v_{min} < v_i(t) < v_{max}$.

$$u_i^*(t) = u_{min}, \quad \forall t \geq t_1. \quad (45)$$

In this case the Hamiltonian is continuous at $t = t_1$ (entry point of the control constrained arc). It follows from (1) that

for $t \geq t_1$

$$v_i^*(t) = u_{min} t + f_i, \quad (46)$$

$$p_i^*(t) = \frac{1}{2} u_{min} t^2 + f_i t + e_i, \quad (47)$$

where f_i and e_i are constants of integration that can be computed easily since we know the speed and position of the vehicle at time $t = t_1$.

5) *Control and State Constraints Become Active, $u_i(t) = u_{min}$ and $v_i(t) = v_{min}$* : Suppose that at time $t = t_2 > t_1$ (exit point of the control constrained arc and entry point of the state variable constrained arc), (46) becomes equal to v_{min} . Then from (1) we have $\dot{v}_i^* = u_i^*(t) = 0$ for $t > t_2$, and the Hamiltonian is discontinuous at $t = t_2$ (corner). Substituting $u_i^*(t) = 0$ for $t > t_2$ into the vehicle dynamics equations (1) we can find the optimal speed and position of each vehicle for $t \geq t_2$, namely

$$v_i^*(t) = v_{min}, \quad (48)$$

$$p_i^*(t) = v_{min} t + r_i, \quad (49)$$

where r_i is the constant of integration that can be computed from the position of the vehicle at $t = t_2^-$.

Since $u_i^*(t) = 0$ for $t > t_2$, at time $t = t_3 > t_2$ (exit point of the corner) the state variable constraint can become inactive again, i.e., $v_{min} < v_i(t) < v_{max}$. The Hamiltonian and co-states are continuous at $t = t_3$. The analysis follows the discussion above at the exit point of the corner in the case where $u_i(t) = u_{max}$ and $v_i(t) = v_{max}$, and the optimal control input, speed, and position are given by (42)- (44).

6) *State Constraints Become Active, $v_i(t) = v_{max}$* : Suppose that at time $t = t_1$ and while $u_{min} < u_i(t) < u_{max}$, (31) becomes equal to v_{max} (entry point of the state variable constrained arc). Then from (1) we have $\dot{v}_i^* = u_i^*(t) = 0$ for $t > t_1$, and the Hamiltonian is discontinuous at $t = t_1$. Substituting $u_i^*(t) = 0$ into the vehicle dynamics equations (1) we can find the optimal speed and position of each vehicle for $t \geq t_1$, namely

$$v_i^*(t) = v_{max}, \quad (50)$$

$$p_i^*(t) = v_{max} t + r_i, \quad (51)$$

where r_i is the constant of integration that can be computed from the position of the vehicle at $t = t_1^-$.

Since $u_i^*(t) = 0$ for $t > t_1$, at time $t = t_3 > t_2$ (exit point of the corner) the state variable constraint can become inactive again, i.e., $v_{min} < v_i(t) < v_{max}$. The Hamiltonian and co-states are continuous at $t = t_3$. The analysis follows the discussion at the exit point of the corner in the case where $u_i(t) = u_{max}$ and $v_i(t) = v_{max}$, and the optimal control input, speed, and position are given by (42)- (44).

7) *State Constraints Become Active, $v_i(t) = v_{min}$* : Suppose that at time $t = t_1$ and while $u_{min} < u_i(t) < u_{max}$, (31) becomes equal to v_{min} (entry point of the state variable constrained arc). Then from (1) we have $\dot{v}_i^* = u_i^*(t) = 0$ for $t > t_1$, and the Hamiltonian is discontinuous at $t = t_1$. If

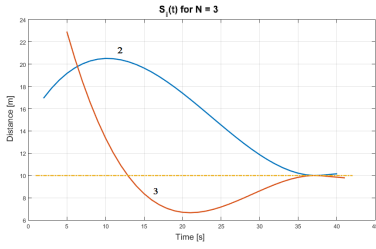


Fig. 3. Example of safety constraint violation by CAV 3 when $\delta = 10$.

follows from (1) that for $t \geq t_1$

$$v_i^*(t) = v_{min}, \quad (52)$$

$$p_i^*(t) = v_{min} t + r_i, \quad (53)$$

where r_i is the constant of integration that can be computed from the position of the vehicle at $t = t_1^-$. The analysis is similar to the case where $u_i(t) = u_{max}$ and $v_i(t) = v_{max}$, and the optimal control input, speed, and position are given by (42)- (44).

Remark 3: The simple nature of the optimal control and states in (30) through (32) makes the online solution of (19) computationally feasible, even with the additional burden of checking for active constraints in Cases 2) through 7). However, there is an additional feature of the solution that we can exploit, i.e., the fact that the control structure for CAV i remains unchanged until an “event” occurs that affects its behavior, e.g., the fact that a constraint becomes active. Therefore, there is no need for a time-driven controller implementation such that $u_i^*(t)$ is repeatedly re-evaluated. Rather, an event-driven controller may be used without affecting its optimality properties under conditions described in [28].

C. Feasibility analysis for safety constraints

As already pointed out in Section III-A, the decentralized problem (19) does not explicitly include the safety constraints (3) and (5). While the latter holds by the construction of $v_i(t_i^m)$ and t_i^m in (11) and (12), the former is not guaranteed to hold for all $t \in [t_i^0, t_i^m]$. We begin with a simple example of how (3) may be violated under the optimal control (30). This is illustrated in Fig. 3 with $\delta = 10$ for two CAVs that follow each other into the same lane in the CZ. We can see that while (3) is eventually satisfied, due to the constraints imposed on the solution of (19) through (5), the controller (30) is unable to maintain (3) throughout the CZ. What is noteworthy in Fig. 3 is that (3) is violated by CAV 3 at an interval which is interior to $[t_3^0, t_3^m]$, i.e., the form of the optimal control solution (30) causes this violation even though the constraint is initially satisfied at $t_3^0 = 5$ in Fig. 3.

Recall that we use k to denote the CAV physically preceding i on the same lane in the CAV, and that $i - 1$ is the CAV preceding i in the FIFO queue associated with the CA. Clearly, $k \leq i - 1$; when $k = i - 1$, then i follows $i - 1$ in the same lane, whereas if $i - 1$ is on a different lane from i , then $k < i - 1$. Using this notation, the following theorem asserts that we can always find initial conditions (t_i^0, v_i^0) which

guarantee the safety constraint (3) holds throughout the CZ under the the decentralized optimal control, even though (3) is not explicitly included in (19).

Theorem 3: There exists a nonempty feasible region $\mathcal{F}_i \subset R^2$ of initial conditions (t_i^0, v_i^0) for CAV i such that, under the decentralized optimal control, $s_i(t) \geq \delta$ holds for all $t \in [t_i^0, t_i^m]$ given the initial and final conditions $t_k^0, v_k^0, t_k^m, v_k^m$ of CAV k .

Proof: To prove the existence of the feasible region, there are two cases to consider, depending on whether any state or control constraint for either CAV i or k becomes active in the CZ.

Case 1: No state or control constraint is active for either k or i over $[t_i^0, t_i^m]$. By using (32), (33) and the definition $s_i(t) = p_k(t) - p_i(t)$, under optimal control we can write

$$\begin{aligned} s_i(t; t_i^0, v_i^0) &= s_i(t, t_i^m, v_i^m, t_k^0, v_k^0, t_k^m, v_k^m; t_i^0, v_i^0) \\ &= A(t, t_i^m, v_i^m, t_k^0, v_k^0, t_k^m, v_k^m; t_i^0, v_i^0)t^3 \\ &\quad + B(t, t_i^m, v_i^m, t_k^0, v_k^0, t_k^m, v_k^m; t_i^0, v_i^0)t^2 \\ &\quad + C(t, t_i^m, v_i^m, t_k^0, v_k^0, t_k^m, v_k^m; t_i^0, v_i^0)t \\ &\quad + D(t, t_i^m, v_i^m, t_k^0, v_k^0, t_k^m, v_k^m; t_i^0, v_i^0), \end{aligned} \quad (54)$$

where A, B, C and D are functions defined over $t \in [t_i^0, t_i^m]$. Recall that CAV k is cruising in the MZ, so that (30) through (32) do not apply for k over $[t_k^m, t_i^m]$ leading to different expressions for A, B, C and D . Therefore, we consider two further subcases, one for $[t_i^0, t_k^m]$ and the other for $[t_k^m, t_i^m]$. For ease of notation, in the sequel we replace (t_i^0, v_i^0) by (τ, v) .

Case 1.1: $t \in [t_i^0, t_k^m]$. In this case, $s_i(t; \tau, v)$ is a cubic polynomial inheriting the cubic structure of (32). We can solve (33) for the coefficients $a_k, b_k, c_k, d_k, a_i, b_i, c_i$ and d_i using the initial and final conditions of CAVs k and i . Then, denoting A, B, C and D as $A_1(\tau, v), B_1(\tau, v), C_1(\tau, v)$ and $D_1(\tau, v)$ for $t \in [t_i^0, t_k^m]$, these are explicitly given by

$$\begin{aligned} A_1(\tau, v) &= \frac{1}{(t_k^0 - t_k^m)^3} (2L + (v_k^m + v_k^0)(t_k^0 - t_k^m)) \\ &\quad - \frac{1}{(\tau - t_i^m)^3} (2L + (v_i^m + v)(\tau - t_i^m)), \end{aligned}$$

$$\begin{aligned} B_1(\tau, v) &= -\frac{1}{(t_k^0 - t_k^m)^3} [3L(t_k^0 + t_k^m) \\ &\quad + (v_k^0(t_k^0 + 2t_k^m) + v_k^m(2t_k^0 + t_k^m))(t_k^0 - t_k^m)] \\ &\quad + \frac{1}{(\tau - t_i^m)^3} [3L(\tau + t_i^m) \\ &\quad + (v(\tau + 2t_i^m) + v_i^m(2\tau + t_i^m))(\tau - t_i^m)], \end{aligned}$$

$$\begin{aligned} C_1(\tau, v) &= \frac{1}{(t_k^0 - t_k^m)^3} [6t_k^0 t_k^m L + [(v_k^0((t_k^m)^2 + 2t_k^0 t_k^m) \\ &\quad + v_k^m((t_k^0)^2 + 2t_k^m t_k^0))](t_k^0 - t_k^m)] \\ &\quad - \frac{1}{(\tau - t_i^m)^3} [6\tau t_i^m L + [(v((t_i^m)^2 + 2\tau t_i^m) \\ &\quad + v_i^m((\tau)^2 + 2t_i^m \tau))](\tau - t_i^m)], \end{aligned}$$

$$\begin{aligned}
D_1(\tau, v) &= \frac{1}{(t_k^0 - t_k^m)^3} [L((t_k^0)^3 - 3(t_k^0)^2 t_k^m) \\
&\quad - (v_k^0 t_k^0 (t_k^m)^2 + v_k^m (t_k^0)^2 t_k^m) (t_k^0 - t_k^m)] \\
&\quad - \frac{1}{(\tau - t_i^m)^3} [L((\tau)^3 - 3(\tau)^2 t_i^m) \\
&\quad - (v\tau (t_i^m)^2 + v_i^m (\tau)^2 t_i^m) (\tau - t_i^m)]. \quad (55)
\end{aligned}$$

Note that in (54) we write $s_i(t; \tau, v)$ (recall that $(t_i^0, v_i^0) \equiv (\tau, v)$) to emphasize the dependence of $s_i(t)$ on these initial conditions for CAV i , i.e., we give a parametric characterization of $s_i(t)$ through (τ, v) . Aside from (τ, v) , the function $s_i(t)$ also depends on two groups of arguments: (i) t_k^0, v_k^0, t_k^m and $v_k^m \equiv v_k(t_k^f) = v_k(t_k^m)$ are quantities associated with CAV k . Since $k < i$, all information related to this CAV is available and is fixed throughout $[t_i^0, t_i^m]$. (ii) t_i^m and $v_i^m \equiv v_i(t_i^f) = v_i(t_i^m)$ are quantities which can also be determined through CAV k or $i - 1$. Specifically, v_i^m is dependent on which subset among $\{\mathcal{R}_i(t), \mathcal{L}_i(t), \mathcal{C}_i(t), \mathcal{O}_i(t)\}$ CAV $i - 1$ belongs to and is determined in (11). Similarly, t_i^m is determined by one of (10), (12) or (13) or though (17) and (6).

To summarize, $s_i(t; \tau, v)$ varies only with t and (τ, v) with all remaining arguments being known to CAV i . First, observing that the first half of each of the coefficient expressions in (55) (which is derived by solving (32) and (33) for CAV k) is a constant fully determined by information provided by CAV k , we can rewrite these as $K_{A_1}, K_{B_1}, K_{C_1}, K_{D_1}$. Therefore, $p_k^*(t)$ in (32) can be expressed as

$$p_k^*(t) = K_{A_1} t^3 + K_{B_1} t^2 + K_{C_1} t + K_{D_1}. \quad (56)$$

Next, the second half of the coefficients can be expressed through polynomials in either τ or v explicitly derived by solving (32) and (33) for CAV i . We will use the notation $P_{X,n}(\tau), P_{X,n}(v)$ to represent polynomials of degree $n = 1, 2, 3$ and $X \in \{A_1, B_1, C_1, D_1\}$. Similarly, we set $Q_3(\tau) = (\tau - t_i^m)^3$. Thus, for the coefficients in Eq. (55), we get

$$A_1(\tau, v) = K_{A_1} + \frac{P_{A_1,1}(\tau)P_{A_1,1}(v)}{Q_3(\tau)},$$

$$B_1(\tau, v) = K_{B_1} + \frac{P_{B_1,2}(\tau)P_{B_1,1}(v)}{Q_3(\tau)},$$

$$C_1(\tau, v) = K_{C_1} + \frac{P_{C_1,3}(\tau) + P_{C_1,2}(\tau)P_{C_1,1}(v)}{Q_3(\tau)},$$

$$D_1(\tau, v) = K_{D_1} + \frac{P_{D_1,3}(\tau) + P_{D_1,2}(\tau)P_{D_1,1}(v)}{Q_3(\tau)}. \quad (57)$$

Note that $p_k^*(t)$ in (56) involves only the K terms, while the analogous cubic polynomial for $p_i^*(t)$ involves only the P and Q terms.

Our goal is to ensure that $s_i(t; \tau, v) \geq \delta$ for all $t \in [\tau, t_k^m]$ (recall that $t_i^0 \equiv \tau$). We can guarantee this by ensuring that $s_i^*(\tau, v) \equiv \min_{t \in [\tau, t_k^m]} \{s_i(t; \tau, v)\} \geq \delta$. Thus, we shift our attention to the determination of $s_i^*(\tau, v)$. We can obtain

expressions for the first and the second derivative of $s_i(t; \tau, v)$, $\dot{s}_i(t; \tau, v)$ and $\ddot{s}_i(t; \tau, v)$ respectively, from (54), as follows:

$$\dot{s}_i(t; \tau, v) = v_k(t) - v_i(t) = 3A_1(\tau, v)t^2 + 2B_1(\tau, v)t + C_1(\tau, v), \quad (58)$$

$$\ddot{s}_i(t; \tau, v) = u_k(t) - u_i(t) = 6A_1(\tau, v)t + 2B_1(\tau, v). \quad (59)$$

Clearly, we can determine $t_i^* \equiv \arg \min_{t \in [\tau, t_k^m]} \{s_i(t; \tau, v)\}$ as the solution of $\dot{s}_i(t; \tau, v) = 0$ with $\ddot{s}_i(t; \tau, v) \geq 0$, unless $s_i^*(\tau, v)$ occurs at the boundaries, i.e., $t_i^* = \tau$ or $t_i^* = t_k^m$. Thus, there are three cases to consider:

Case 1.1.A: $t_i^* = \tau$. In this case,

$$\begin{aligned}
s_i^*(\tau, v) &= s_i(\tau; \tau, v) \quad (60) \\
&= A_1(\tau, v)\tau^3 + B_1(\tau, v)\tau^2 + C_1(\tau, v)\tau + D_1(\tau, v) \geq \delta
\end{aligned}$$

and we can satisfy $s_i(\tau, v) \geq \delta$ for any v as long as a feasible τ is determined. Since at $t = \tau$, we have $p_i(\tau) = 0$ and using the definition of $s_i(t) = p_k(t) - p_i(t)$ and (56), we get

$$s_i(\tau) = p_k^*(\tau) = K_{A_1}\tau^3 + K_{B_1}\tau^2 + K_{C_1}\tau + K_{D_1}.$$

Observe that if

$$p_k(\tau) \geq \delta$$

then CAV i enters the CZ at a safe distance from its preceding CAV k and since $t_i^* = \tau$, we have $s_i(t; \tau, v) \geq \delta$ for all $t \in [\tau, t_k^m]$. Thus, it suffices to select

$$\tau \geq t_k^\delta \quad (61)$$

where t_k^δ is the smallest real root of $p_k(\tau) - \delta = 0$.

Case 1.1.B: $t_i^* = t_k^m$. In this case,

$$\begin{aligned}
s_i^*(\tau, v) &= s_i(t_k^m; \tau, v) \quad (62) \\
&= A_1(\tau, v)(t_k^m)^3 + B_1(\tau, v)(t_k^m)^2 + C_1(\tau, v)t_k^m \\
&\quad + D_1(\tau, v) \geq \delta
\end{aligned}$$

Thus, the feasibility region \mathcal{F}_i is defined by all (τ, v) such that $s_i(t_k^m; \tau, v) - \delta \geq 0$ in the (τ, v) space.

Case 1.1.C: $t_i^* = t_1 \in (\tau, t_k^m)$. This case only arises if the determinant $\mathcal{D}_i(\tau, v)$ of (58) is positive, i.e.,

$$\mathcal{D}_i(\tau, v) = 4B_1(\tau, v)^2 - 12A_1(\tau, v)C_1(\tau, v) > 0 \quad (63)$$

and we get

$$t_1 = \frac{-2B_1(\tau, v) \pm \sqrt{\mathcal{D}_i(\tau, v)}}{6A_1(\tau, v)} \quad (64)$$

In addition, we must have

$$\tau < t_1 < t_k^m, \quad \dot{s}_i(t_1; \tau, v) = 0, \quad \ddot{s}_i(t_1; \tau, v) \geq 0 \quad (65)$$

Therefore, the feasibility region \mathcal{F}_i is defined by all (τ, v) such that

$$\begin{aligned}
s_i^*(\tau, v) &= s_i(t_1; \tau, v) \\
&= A_1(\tau, v)(t_1)^3 + B_1(\tau, v)(t_1)^2 + C_1(\tau, v)t_1 \\
&\quad + D_1(\tau, v) \geq \delta
\end{aligned} \quad (66)$$

in conjunction with (64)-(65).

Case 1.2: $t \in [t_k^m, t_i^m]$. Over this interval, $v_k(t) = v_k^m$ by Assumption 2. Therefore, (30)-(32) no longer apply: (30) becomes $u_k^*(t) = 0$, (31) becomes $v_k^*(t) = v_k^m$ and (32) becomes $p_k^*(t) = L + v_k^m(t - t_k^m)$. Evaluating $s_i(t) = p_k(t) - p_i(t)$ in this case yields the following coefficients in (55):

$$\begin{aligned} A_2(\tau, v) &= -\frac{1}{(\tau - t_i^m)^3} (2L + (v_i^m + v)(\tau - t_i^m)), \\ B_2(\tau, v) &= \frac{1}{(\tau - t_i^m)^3} [3L(\tau + t_i^m) + (v(\tau + 2t_i^m) \\ &\quad + v_i^m(2\tau + t_i^m))(\tau - t_i^m)], \\ C_2(\tau, v) &= v_k^m - \frac{1}{(\tau - t_i^m)^3} [6\tau t_i^m L + [(v((t_i^m)^2 + 2\tau t_i^m) \\ &\quad + v_i^m((\tau)^2 + 2t_i^m \tau))](\tau - t_i^m)], \\ D_2(\tau, v) &= L - v_k^m t_k^m - \frac{1}{(\tau - t_i^m)^3} [L((\tau)^3 - 3(\tau)^2 t_i^m) \\ &\quad - (v\tau(t_i^m)^2 + v_i^m(\tau)^2 t_i^m)(\tau - t_i^m)]. \end{aligned} \quad (67)$$

It follows that $K_{A_1}, K_{B_1}, K_{C_1}$ and K_{D_1} in (57) should be modified accordingly, giving $K_{A_2} = K_{B_2} = 0$, $K_{C_2} = v_k^m$ and $K_{D_2} = L - v_k^m t_k^m$. Since we are assuming that no control or state constraints are active for CAV i , the designated final time t_i^m under optimal control satisfies (12), i.e., $s_i(t_k^m) = \delta$. Thus, we only need to consider the subcase where $s_i^*(\tau, v)$ occurs in (t_k^m, t_i^m) and we have

$$t_i^* = t_2, \quad t_2 \in (t_k^m, t_i^m).$$

Proceeding as in *Case 1.1.C*, the feasibility region \mathcal{F}_i is defined by all (τ, v) such that

$$\begin{aligned} s_i^*(\tau, v) &= s_i(t_2; \tau, v) \\ &= A_2(\tau, v)(t_2)^3 + B_2(\tau, v)(t_2)^2 + C_2(\tau, v)t_2 \\ &\quad + D_2(\tau, v) \geq \delta \end{aligned} \quad (68)$$

in conjunction with (64)-(65), with A_1, B_1, C_1 and D_1 replaced by A_2, B_2, C_2 and D_2 , and with $\tau < t_1 < t_k^m$ replaced by $t_k^m < t_2 < t_i^m$.

Case 2: At least one of the state and control constraints is active over $[\tau, t_i^m]$. As discussed in Section IV-B, there are several cases to consider when state and/or control constraints are active. Since one or both CAVs k and i may experience an active constraint, all different combinations need to be considered. We analyze a few in what follows since it is clear that the remaining cases are handled in a similar fashion.

Case 2.1: $v_k^*(t) = v_{max}$ over an optimal trajectory arc, while CAV i is unconstrained. In this case, (30)-(32) no longer apply for CAV k and the coefficients in (55) are affected similar to *Case 1.2*, except that the fixed speed v_k^m is now v_{max} .

First, consider the interval $[\tau, t_k^m]$. Following the Hamiltonian analysis in Section IV-B, let t_k^I be the time CAV k enters the constrained arc with $v_k^*(t) = v_{max}$ and t_k^E be the time it exits this arc (see subfigure (a) in Fig. 4). The trajectory of CAV k consists of three arcs as follows. First, for $t \in [\tau, t_k^I]$, A_1, B_1, C_1 and D_1 are defined exactly as in (55). Second,

for $t \in [t_k^I, t_k^E]$, (30)-(32) are replaced by $u_k^*(t) = 0$, and $v_k^*(t) = v_{max}$ and (32) becomes $p_k^*(t) = p_k(t_k^I) + v_{max}(t - t_k^I)$, where $p_k(t_k^I)$ can be determined before CAV i enters the CZ. The form of the coefficients in (55) is modified the same way as in (67), with v_k^m and L replaced by v_{max} and $p_k(t_k^I)$. It follows that $K_{A_1}, K_{B_1}, K_{C_1}$ and K_{D_1} in (57) should also be modified accordingly, with $K_{A_2} = K_{B_2} = 0$, $K_{C_2} = v_{max}$ and $K_{D_2} = p_k(t_k^I) - v_{max}t_k^I$. The final arc is for $t \in [t_k^E, t_i^m]$, when CAV k returns to an unconstrained arc. The form of the coefficients in (55) does not change, except that A_1, B_1, C_1 and D_1 should be replaced by A_3, B_3, C_3 and D_3 since the value of the coefficients may differ for different unconstrained arcs.

As in *Case 1.1*, we next consider $t_i^* \equiv \arg \min_{t \in [\tau, t_k^m]} \{s_i(t; \tau, v)\}$ and there are three cases.

Case 2.1.A: $t_i^* = \tau$. As in *Case 1.1.A*, it suffices to select $\tau \geq t_k^\delta$ where t_k^δ is the smallest real root of $p_k^*(\tau) = \delta$.

Case 2.1.B: $t_i^* = t_k^m$. As in *Case 1.1.B*, the feasibility region \mathcal{F}_i is defined by all (τ, v) such that $s_i(t_k^m; \tau, v) - \delta \geq 0$ in the (τ, v) space, with A_1, B_1, C_1 and D_1 being replaced by A_3, B_3, C_3 and D_3 .

Case 2.1.C: $t_i^* = t_1 \in (\tau, t_k^m)$. This case may only arise for $t \in (\tau, t_k^I)$. As in *Case 1.1.C*, the feasibility region \mathcal{F}_i is defined by

$$\begin{aligned} s_i^*(\tau, v) &= s_i(t_1; \tau, v) \\ &= A_1(\tau, v)(t_1)^3 + B_1(\tau, v)(t_1)^2 + C_1(\tau, v)t_1 \\ &\quad + D_1(\tau, v) \geq \delta \end{aligned} \quad (69)$$

in conjunction with (64)-(65) with $\tau < t_1 < t_k^m$ being replaced by $\tau < t_1 < t_k^I$.

For $t \in [t_k^m, t_i^m]$, the analysis is exactly the same as the way we handle *Case 1.2*, with A_2, B_2, C_2 and D_2 being replaced by A_4, B_4, C_4 and D_4 . The feasibility region \mathcal{F}_i is defined by

$$\begin{aligned} s_i^*(\tau, v) &= s_i(t_2; \tau, v) \\ &= A_4(\tau, v)(t_2)^3 + B_4(\tau, v)(t_2)^2 + C_4(\tau, v)t_2 \\ &\quad + D_4(\tau, v) \geq \delta \end{aligned} \quad (70)$$

in conjunction with (64)-(65).

Case 2.2: CAV k is unconstrained and $u_i^*(t) = u_{min}$ over an optimal trajectory arc. Since there are many subcases and each can be similarly handled, we only consider one subcase where CAV i enters the constrained arc at t_k^m (see subfigure (b) in Fig. 4).

Since both CAV k and i are unconstrained in $[\tau, t_k^m]$, the form of the coefficients in (55) does not change, and the feasibility region for *Cases 2.2.A, 2.2.B* and *2.2.C* can be derived in the same way as *Case 1.1.A, 1.1.B* and *1.1.C*. For $t \in [t_k^m, t_i^m]$, CAV i is decelerating at a constant value $u_i^*(t) = u_{min}$. Thus, (30)-(32) are replaced by $u_i^*(t) = u_{min}$, $v_i^*(t) = v_i(t_k^m) + u_{min}(t - t_k^m)$ and $p_i^*(t) = L + v_i(t)(t - t_k^m)$, where $v_i(t_k^m)$ can be determined given (τ, v) . The coefficients

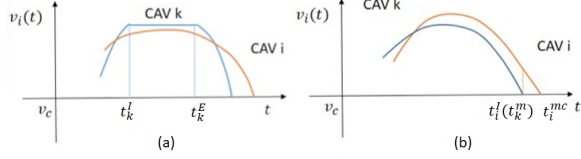


Fig. 4. Cases when the state and/or control constraints are active.

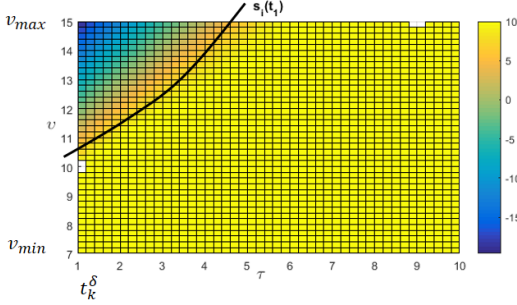


Fig. 5. Feasible and infeasible region for Case 1.I.C.

in (55) are modified as follows:

$$\begin{aligned}
 A_2(\tau, v) &= 0, \\
 B_2(\tau, v) &= -\frac{1}{2}u_{min}, \\
 C_2(\tau, v) &= v_k^m - v_i(t_k^m) + u_{min}t_k^m, \\
 D_2(\tau, v) &= -v_k^m t_k^m.
 \end{aligned} \tag{71}$$

For $t \in [t_k^m, t_i^m]$, $v_i^*(t) > v_k^*(t)$ and CAV i keeps decelerating until it reaches $v_i^m = v_k^m$. Therefore, s_i^* may only occur at t_i^m and we have

$$\begin{aligned}
 s_i^*(\tau, v) &= s_i(t_i^m; \tau, v) \\
 &= A_2(\tau, v)(t_i^m)^3 + B_2(\tau, v)(t_i^m)^2 + C_2(\tau, v)t_i^m \\
 &\quad + D_2(\tau, v) \geq \delta
 \end{aligned} \tag{72}$$

Thus, the feasibility region \mathcal{F}_i is defined by all (τ, v) such that $s_i(t_i^m; \tau, v) - \delta \geq 0$ in the (τ, v) space.

All remaining cases are similarly handled and in each case a feasibility region \mathcal{F}_i is defined by all (τ, v) satisfying an inequality of the form $s_i(\sigma; \tau, v) - \delta \geq 0$ for an appropriate value of σ and coefficients in (54).

To complete the proof, we show that feasibility region \mathcal{F}_i is always nonempty. This is easily established by considering a point (τ, v) such that $v_{min} < v < v_{max}$ (which is possible by Assumption 1) and $\tau = t_k^f$: since $p_k^*(t_k^f) = L + S$ and $p_i^*(\tau) = 0$, it follows that $s_i(\tau) > S > \delta$. Obviously, any such (τ, v) is feasible. ■

To illustrate the feasible region and provide some intuition, we give a numerical example where Case 1.I.C applies (see Fig. 5), with $\delta = 10$, $L = 400$, and CAV k is the first vehicle in the CZ and is driving at the constant speed $v_k^m = 10$. The colorbar in Fig. 5 indicates the value of $s_i^*(t)$ and the yellow

region, determined by (66), represents the feasible region, while the non-yellow region represents the infeasible region. The black curve is the boundary between the two regions and is not linear in general. This boundary curve shifts depending on the different cases we have considered in the proof of Theorem 3. This example also illustrates that we can always find a nonempty feasible region since we can select points to the right of the curve corresponding to CAV i entry times in the CZ which can be arbitrarily large.

For any set of initial conditions which are feasible, each case gives an optimal control solution, possibly with a constrained arc. The case which applies depends on the choice of initial conditions. In other words, our analysis provides a map from the feasible region to a set of optimal controls for CAV i which all satisfy the safety inequality. Theorem 3 asserts that as long as we can drive the CAV to a feasible initial point, there exists a solution satisfying the safety inequality over the entire CZ and MZ which may or may not include a constrained arc. The feasibility enforcement analysis for the vehicles to satisfy such initial conditions is discussed in [27].

V. SIMULATION RESULTS

To evaluate the effectiveness of the proposed solution, we simulated an intersection of two roads with four lanes, two lanes in each direction, i.e., vehicles travel from east to west and west to east in one road, and from south to north and north to south in the other one. Vehicles are not allowed to make turns or change lanes. The length of the MZ, S , is 30 m and the length of the CZ, L , is 400 m. The minimum safe distance, δ , between two vehicles is 10 m. The maximum and minimum speed limits are 18 m/s and 12 m/s respectively. We considered the following three case studies: (1) coordination of 28 vehicles (14 on each road), (2) coordination of 56 vehicles (28 on each road), and (3) coordination of 470 vehicles. For the first two studies we used MATLAB and for the third one VISSIM.

The proposed solution was compared to a baseline scenario, where the intersection has traffic lights with fixed switching times. To quantify the impact of the vehicle coordination on fuel consumption, we used the polynomial metamodel proposed in [29] that yields vehicle fuel consumption as a function of the speed, $v(t)$, and control input, $u(t)$

$$\dot{f}_v = \dot{f}_{cruise} + \dot{f}_{accel} \tag{73}$$

where $\dot{f}_{cruise} = w_0 + w_1v(t) + w_2v^2(t) + w_3v^3(t)$ yields the fuel consumed by a vehicle traveling at a constant speed $v(t)$ and $\dot{f}_{accel} = u(t) \cdot (r_0 + r_1v(t) + r_2v^2(t))$ is the additional fuel consumption due to acceleration $u(t)$. The polynomial coefficients w_n , $n = 0, \dots, 3$ and r_m , $m = 0, 1, 2$ are calculated from experimental data. For the case studies we considered in this paper, all vehicles are the same with the parameters reported in [29], where the vehicle mass is $M_v = 1,200$ kg, the drag coefficient is $C_D = 0.32$, the air density is $\rho_a = 1.184$ km/m³, the frontal area is $A_f = 2.5$ m², and the rolling resistance coefficient is $\mu = 0.015$.

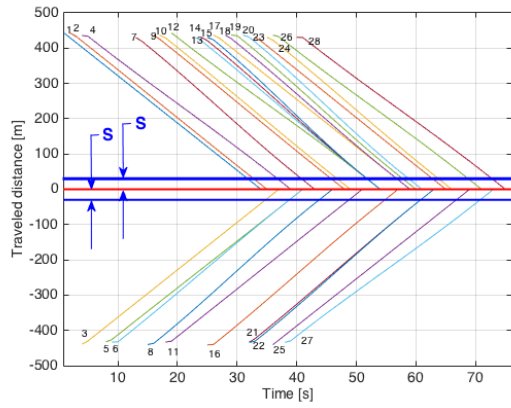


Fig. 6. Vehicle coordination at the intersection.

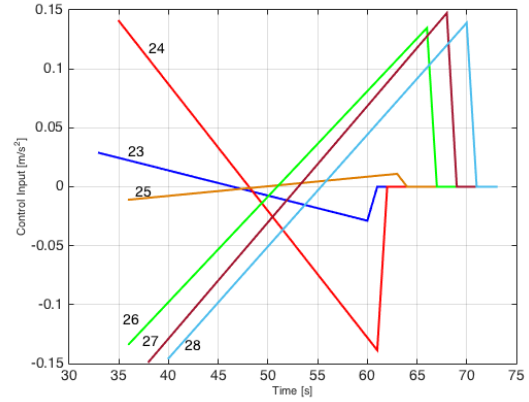


Fig. 8. Control input signal of the last six vehicles in the queue.

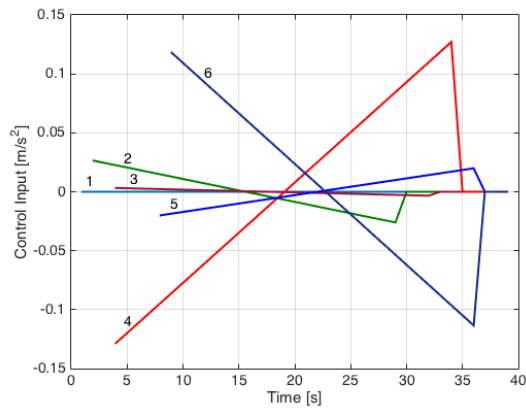


Fig. 7. Control input signal of the first six vehicles in the queue.

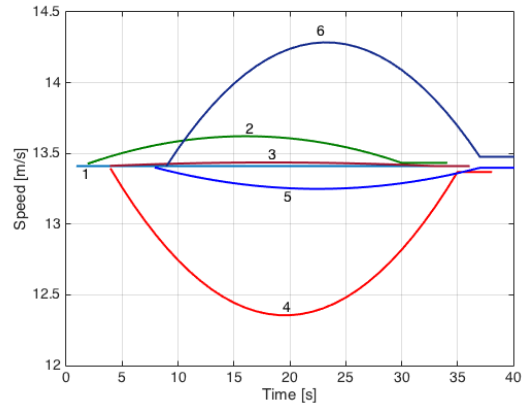


Fig. 9. Speed of the first six vehicles in the queue.

For the first case study, the trajectory of the position of each vehicle crossing the MZ is shown in Fig. 6. Vehicles traveling on the same road but on different lanes can cross the MZ at the same time, e.g., a) #5 and #6 and b) #12, #13, #14, #15. Vehicles on the same road and same lane cross the MZ within the safe distance δ , e.g., a) #1 and #2, b) #9 and #10, c) #18, #19 and #20, and d) #23 and #24. The control input for the first and last six vehicles in the queue is shown in Fig. 7 and Fig. 8, while the corresponding speed profiles are shown in Fig. 9 and Fig. 10 respectively. The first vehicle is not constrained and travels with a constant speed (Fig. 9). The second vehicle is on the same lane (Fig. 6) and accelerates until it reaches the safe distance δ with the first vehicle. The third vehicle accelerates as required to enter the MZ right after second vehicle, while the fourth and fifth have to decelerate initially until the preceding vehicles cross the MZ. The coordination of vehicles yield 54.7% reduction in fuel consumption and 17.3 % reduction in total travel time compared to the case with traffic lights.

In the second and third case studies, we considered the same intersection. Fuel consumption improvement was 65.1% and 52 % respectively while the travel time was improved by 5.8%

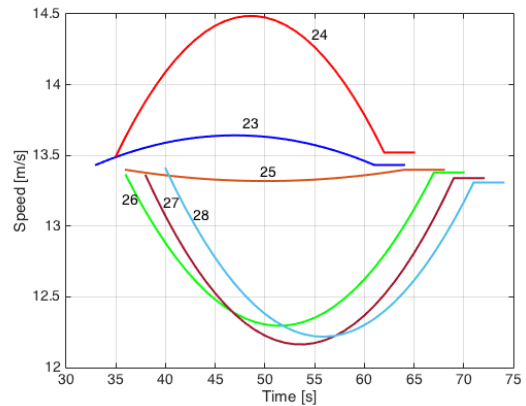


Fig. 10. Speed of the last six vehicles in the queue.

and 21%. The fuel consumption improvement is due to the following reasons: (1) the vehicles do not come to a full stop, thereby conserving momentum, and (2) each vehicle uses its optimal acceleration/deceleration inside the CZ.

VI. CONCLUDING REMARKS AND FUTURE WORK

We considered the problem of optimally controlling CAVs crossing an urban intersection without any explicit traffic signaling. Our objective was to maximize the traffic throughput at the intersection using the minimum acceleration/deceleration of each vehicle, in terms of fuel consumption, under the hard safety constraints to avoid rear-end and lateral collisions. We formulated the centralized problem and showed that (1) the solution of this problem provides the times required for individual CAVs to cross the intersection, and (2) the centralized problem becomes, under certain conditions, equivalent to a decentralized framework whereby each CAV minimizes its energy consumption subject to the throughput-maximizing timing constraints. We presented a complete analytical solution of these decentralized problems and derived conditions under which feasible solutions satisfying all safety constraints always exist.

In our decentralized framework, we considered full penetration of identical CAVs having access to perfect information, i.e., information without any errors and/or delays, while we did not consider lane changing or turns in the intersection or pedestrians. Ongoing research is considering lane changing and turns in the intersection with a diverse set of CAVs and exploring the associated tradeoffs between maximizing the throughput of an intersection and fuel consumption of each individual vehicle. Ongoing research is also investigating the implications of the proposed approach to adjacent intersections [22] and considering a feasibility enforcement analysis [27] to ensure that each CAV starts from a feasible state and control once it enters the control zone. The fact that the control structure for each CAV remains unchanged until an “event” occurs that affects its behavior is an additional feature of the solution that is being exploited and which will eventually lead to event-driven controllers.

An important direction for future research is to consider different penetrations of CAVs, which can alter significantly the efficiency of the entire system. One particular question that still remains unanswered is “what is the minimum number of vehicles that need to be connected so as to start realizing potential benefits?” The assumption of perfect information seems to impose barriers in a potential implementation and deployment of the proposed framework. Although it is relatively straightforward to extend our results in the case that this assumption is relaxed, future research should investigate the implications of having information with errors and/or delays to the system behavior.

REFERENCES

[1] B. Schrank, B. Eisele, T. Lomax, and J. Bak, “2015 Urban Mobility Scorecard,” Texas A& M Transportation Institute, Tech. Rep., 2015.

- [2] A. A. Malikopoulos and J. P. Aguilar, “An Optimization Framework for Driver Feedback Systems,” *IEEE Transactions on Intelligent Transportation Systems*, vol. 14, no. 2, pp. 955–964, 2013.
- [3] R. Margiotta and D. Snyder, “An agency guide on how to establish localized congestion mitigation programs,” U.S. Department of Transportation. Federal Highway Administration, Tech. Rep., 2011.
- [4] S. E. Shladover, C. A. Desoer, J. K. Hedrick, M. Tomizuka, J. Walrand, W.-B. Zhang, D. H. McMahon, H. Peng, S. Sheikholeslam, and N. McKeown, “Automated vehicle control developments in the PATH program,” *IEEE Transactions on Vehicular Technology*, vol. 40, no. 1, pp. 114–130, 1991.
- [5] R. Rajamani, H.-S. Tan, B. K. Law, and W.-B. Zhang, “Demonstration of integrated longitudinal and lateral control for the operation of automated vehicles in platoons,” *IEEE Transactions on Control Systems Technology*, vol. 8, no. 4, pp. 695–708, 2000.
- [6] R. Tachet, P. Santi, S. Sobolevsky, L. I. Reyes-Castro, E. Frazzoli, D. Helbing, and C. Ratti, “Revisiting street intersections using slot-based systems,” *PLOS ONE*, vol. 11, no. 3, 2016.
- [7] M. Athans, “A unified approach to the vehicle-merging problem,” *Transportation Research*, vol. 3, no. 1, pp. 123–133, 1969.
- [8] W. Levine and M. Athans, “On the optimal error regulation of a string of moving vehicles,” *IEEE Transactions on Automatic Control*, vol. 11, no. 3, pp. 355–361, 1966.
- [9] P. Varaiya, “Smart cars on smart roads: problems of control,” *IEEE Transactions on Automatic Control*, vol. 38, no. 2, pp. 195–207, 1993.
- [10] K. Dresner and P. Stone, “Multiagent traffic management: a reservation-based intersection control mechanism,” in *Proceedings of the Third International Joint Conference on Autonomous Agents and Multiagents Systems*, 2004, pp. 530–537.
- [11] —, “A Multiagent Approach to Autonomous Intersection Management,” *Journal of Artificial Intelligence Research*, vol. 31, pp. 591–653, 2008.
- [12] A. de La Fortelle, “Analysis of reservation algorithms for cooperative planning at intersections,” *13th International IEEE Conference on Intelligent Transportation Systems*, pp. 445–449, Sept. 2010.
- [13] S. Huang, A. Sadek, and Y. Zhao, “Assessing the Mobility and Environmental Benefits of Reservation-Based Intelligent Intersections Using an Integrated Simulator,” *IEEE Transactions on Intelligent Transportation Systems*, vol. 13, no. 3, pp. 1201,1214, 2012.
- [14] I. H. Zohdy, R. K. Kamalanathsharma, and H. Rakha, “Intersection management for autonomous vehicles using iCACC,” *2012 15th International IEEE Conference on Intelligent Transportation Systems*, pp. 1109–1114, 2012.
- [15] F. Yan, M. Dridi, and A. El Moudni, “Autonomous vehicle sequencing algorithm at isolated intersections,” *2009 12th International IEEE Conference on Intelligent Transportation Systems*, pp. 1–6, 2009.
- [16] F. Zhu and S. V. Ukkusuri, “A linear programming formulation for autonomous intersection control within a dynamic traffic assignment and connected vehicle environment,” *Transportation Research Part C: Emerging Technologies*, Jan. 2015.
- [17] J. Lee, B. B. Park, K. Malakorn, and J. J. So, “Sustainability assessments of cooperative vehicle intersection control at an urban corridor,” *Transportation Research Part C: Emerging Technologies*, vol. 32, pp. 193–206, 2013.
- [18] K.-D. Kim and P. Kumar, “An MPC-Based Approach to Provable System-Wide Safety and Liveness of Autonomous Ground Traffic,” *IEEE Transactions on Automatic Control*, vol. 59, no. 12, pp. 3341–3356, 2014.
- [19] D. Miculescu and S. Karaman, “Polling-Systems-Based Control of High-Performance Provably-Safe Autonomous Intersections,” in *53rd IEEE Conference on Decision and Control*, 2014.
- [20] J. Alonso, V. Milanés, J. Pérez, E. Onieva, C. González, and T. de Pedro, “Autonomous vehicle control systems for safe crossroads,” *Transportation Research Part C: Emerging Technologies*, vol. 19, no. 6, pp. 1095–1110, Dec. 2011.
- [21] A. Colombo and D. Del Vecchio, “Least Restrictive Supervisors for Intersection Collision Avoidance: A Scheduling Approach,” *IEEE Transactions on Automatic Control*, vol. Provisiona, 2014.
- [22] Y. Zhang, A. A. Malikopoulos, and C. G. Cassandras, “Optimal control and coordination of connected and automated vehicles at urban traffic intersections,” in *Proceedings of the American Control Conference*, 2016, pp. 6227–6232.
- [23] J. Rios-Torres and A. A. Malikopoulos, “A Survey on the Coordination of Connected and Automated Vehicles at Intersections and Merging at

- Highway On-Ramps,” *IEEE Transactions on Intelligent Transportation Systems*, 2016 (forthcoming).
- [24] J. Rios-Torres, A. A. Malikopoulos, and P. Pisu, “Online Optimal Control of Connected Vehicles for Efficient Traffic Flow at Merging Roads,” in *2015 IEEE 18th International Conference on Intelligent Transportation Systems*, 2015, pp. 2432–2437.
- [25] J. Rios-Torres and A. A. Malikopoulos, “Automated and Cooperative Vehicle Merging at Highway On-Ramps,” *IEEE Transactions on Intelligent Transportation Systems*, 2016 (forthcoming).
- [26] A. A. Malikopoulos, P. Y. Papalambros, and D. N. Assanis, “Online identification and stochastic control for autonomous internal combustion engines,” *Journal of Dynamic Systems, Measurement, and Control*, vol. 132, no. 2, pp. 024 504–024 504, 2010.
- [27] Y. Zhang, C. G. Cassandras, and A. A. Malikopoulos, “Optimal control of connected automated vehicles at urban traffic intersections: A feasibility enforcement analysis,” in *2017 American Control Conference*, 2017,- arXiv:1608.04311 (in review).
- [28] M. Zhong and C. G. Cassandras, “Asynchronous distributed optimization with event-driven communication,” *IEEE Transactions on Automatic Control*, vol. 55, no. 12, pp. 2735–2750, 2010.
- [29] M. Kamal, M. Mukai, J. Murata, and T. Kawabe, “Model Predictive Control of Vehicles on Urban Roads for Improved Fuel Economy,” *IEEE Transactions on Control Systems Technology*, vol. 21, no. 3, pp. 831–841, 2013.